We examined the regulatory potential of extremely small (0.3*g*, where *g* is the Earth's gravitational field), high-frequency (30 Hz) mechanical accelerations by subjecting the hindlimbs of adult (6–8-year-old) female sheep (Warhill, intact ewes) to a ground-based vertical oscillation[7] for 20 min per day for 5 days a week. When the animals were not being treated, they joined the controls to roam freely over a pasture area. We used strain gauges attached to the animals' tibia bone to calibrate the device: these showed that the peak-to-peak amplitude of the strain generated was about 5 microstrain, which is 0.1% of the strain magnitude that is known to cause yield-failure in bone[8].

After 1 year of this mechanical-stimulation regime, the density of trabecular bone in the proximal femur, as quantified by computer tomography, was 34.2% greater in experimental sheep than in controls ($P < 0.01$; Table 1). This strong anabolic response was substantiated by undecalcified bone histology of the same region, which revealed a 32% increase in trabecular bone volume, a 45% increase in trabecular mesh number (Fig. 1) and a 36% reduction in mesh spacing, indicating an increase in the mean width of each trabecular element and the addition of new trabeculae.

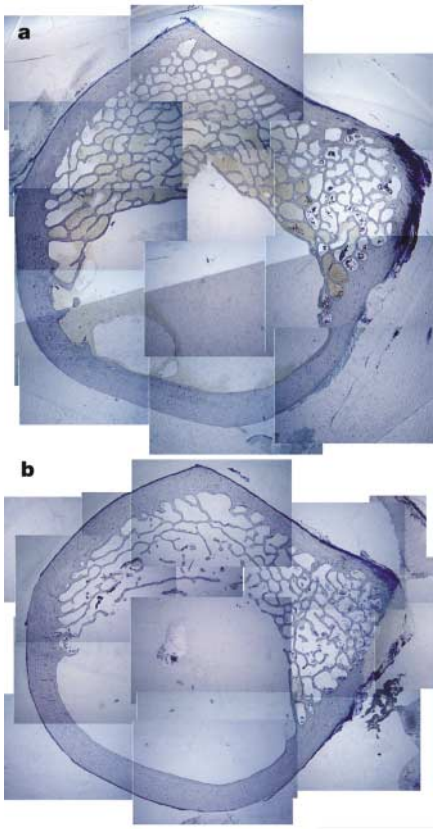

Figure 1 Montages of photomicrographs of the proximal sheep femur used for static histomorphometric evaluation after 1 year of exposure (20 min per day) to a 0.3*g*, 30-Hz mechanical stimulus. **a, b,** There is 32% more trabecular bone in the proximal femur of experimental animals (**a**) compared with age-matched controls (**b**) ($P < 0.04$).

Table 1 Proximal-femur parameters of control and stimulated sheep

	Control	Experimental	Difference	P
Animal mass (kg)	71.1 ± 7.1	70.3 ± 9.4	−1.1%	n.s.
Total density (gm cm^{-3})	466 ± 60	496 ± 53	+6.5%	< 0.1
Trabecular density (gm cm^{-3})	169 ± 37	227 ± 56	+34.2%	< 0.01
Bone volume/total volume (%)	15.2 ± 4.1	20.1 ± 4.8	+32%	< 0.04
Trabecular spacing (μm)	1,170 ± 124	756 ± 97	−36%	< 0.02
Trabecular number (trabeculae mm^{-2})	0.82 ± 0.16	1.19 ± 0.18	+45%	< 0.01
Bone-formation rate (μm^2 mm^{-1})	8.4 ± 12.7	17.9 ± 16.3	+113%	< 0.2
Mineralizing surface (%)	2.6 ± 0.16	6.34 ± 5.14	+144%	< 0.1

Animal mass and envelope-specific bone density (determined by quantitative computer tomography) of the proximal femur after 12 months of low-level mechanical stimulation. Also shown are indices of static and dynamic histomorphometry of the proximal femur. Although 'whole-bone' parameters of the proximal femur show only a limited tendency to be influenced by mechanical stimuli ($P = 0.1$), the increase in treated animals compared with controls is over 30% for trabecular bone alone ($P < 0.01$). One control was lost over the course of study for reasons not associated with the protocol. Nine animals were evaluated in the experimental group, with eight controls. All evaluations were made without knowledge of whether the animals were control or experimental.

We found that this low-level mechanical stimulation increased the rate of bone formation 2.1-fold ($P < 0.2$) and the mineralizing surface 2.4-fold ($P < 0.1$). This anabolic effect was highly specific to cancellous (porous) bone, as there was no significant histomorphometric change in any of the cortical bone parameters. We detected no difference in any bone index in the radius of either control or experimental animals (for example, mineral density was 0.6% less than controls; not statistically significant), indicating that the anabolic effect was specific to the region of the skeleton that was subjected to the mechanical signal.

Mechanical strain in the skeleton is a product of functional load-bearing — as seen, for example, in the mandible of the macaque[9] and the tibia of the alligator[10]. In addition to the large-amplitude strains typically associated with functional activity, a strain signal, much less than 5 microstrain in amplitude, arises through muscular activity in the frequency band 10–50 Hz (ref. 11). Generation of this small-amplitude, high-frequency muscle 'vibration' persists through even such passive activities as standing.

Skeletal morphology may therefore be sculpted by omnipresent, low-level muscle activity as well as by the peak impacts inherent in load-bearing. In terms of clinical relevance, the strong bone-generating capacity of these small signals suggests that biomechanical intervention might help to strengthen bone in osteoporosis sufferers without the side-effects associated with pharmacological treatment. In addition to being non-invasive and inducing a therapeutic response from the bone tissue itself, low-intensity mechanical signals incorporate all aspects of a complex remodelling cycle[12] and ultimately stimulate formation of lamellar bone[13] to improve bone quantity and quality.

Clinton Rubin*, A. Simon Turner†, Steven Bain‡, Craig Mallinckrodt†, Kenneth McLeod*

**Musculo-Skeletal Research Laboratory, Department of Biomedical Engineering, State University of New York, Stony Brook, New York 11794-2580, USA*
e-mail: clinton.rubin@sunysb.edu
†Department of Clinical Sciences, Colorado State University, Fort Collins, Colorado 80523, USA
‡Skeletech Inc., Bothell, Washington 98021, USA

1. Wolff, J. *The Law of Bone Remodeling* (transl. Maquet, P. & Furlong, R.) (Springer, Berlin, 1986).
2. Frost, H. *Anat. Rec.* **26,** 403–413 (1990).
3. Burr, D., Martin, R., Schaffler, M. & Radin, E. *J. Biomech.* **18,** 189–200 (1985).
4. Rubin, C. & Lanyon, L. *J. Exp. Biol.* **101,** 187–211 (1982).
5. Schaffler, M., Radin, E. & Burr, D. *Bone* **11,** 321–326 (1990).
6. Huang, R., McLeod, K. & Rubin, C. *J. Gerontol.* **54,** 352–357 (1999).
7. Fritton, J., Rubin, C., Qin, Y. & McLeod, K. *Ann. Biomed. Eng.* **25,** 831–839 (1997).
8. Carter, D., Harris, W., Vasu, R. & Caler, W. *Am. Soc. Mech. Eng.* **45,** 81–95 (1981).
9. Hylander, W., Ravosa, M., Ross, C. & Johnson, K. *Am. J. Phys. Anthropol.* **107,** 257–271 (1998).
10. Blob, R. & Biewener, A. *J. Exp. Biol.* **202,** 1023–1046 (1999).
11. Fritton, S., McLeod, K. & Rubin, C. *J. Biomech.* **33,** 317–326 (2000).
12. Bain, S. & Rubin, C. *J. Bone Miner. Res.* **5,** 1069–1075 (1990).
13. Rubin, C., Gross, T., McLeod, K. & Bain, S. *J. Bone Miner. Res.* **10,** 488–495 (1995).

Vision

Realignment of cones after cataract removal

Through unique observations of an adult case of bilateral congenital cataract removal[1], we have found evidence that retinal photoreceptors will swiftly realign towards the brightest regions in the pupils of the eye. Cones may be phototropic, actively orientating themselves towards light like sunflowers in a field.

For 40 years, one of us (P.D.) lived with an unusual pupil configuration caused by congenital bilateral cataracts, first diagnosed at three years of age. The cataracts were managed by using a twice-weekly application of atropine, which dilated P.D.'s pupils to produce roughly annular (ring-shaped), clear regions around the dense nuclear cataracts. Because his optics were so poor (he was far-sighted, astigmatic and incapable of accommodation), P.D. squinted continuously as an adaptation, particularly for close work. His eyelids thus horizontally cropped each annulus at the top and bottom, leaving two clear entry points for light

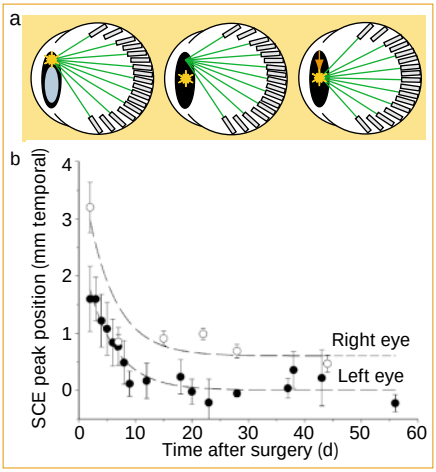

Figure 1 Photoreceptor alignment in P.D.'s eyes before and after cataract removal. **a,** Schematic horizontal cross-sections through P.D.'s eyes. Left, before surgery: receptors were aligned (green lines) with the brightest pupil location (orange 'sun') in the temporal margins; middle, immediately after surgery: the brightest location shifted to the pupil centres, but the receptors retained their skewed alignment; right, after 10 days: receptors realigned with the bright pupil centres (arrow depicts shifts measured in **b**). **b,** Photoreceptor alignment in the pupil plane after cataract removal, as inferred from Stiles–Crawford effect (SCE I) peaks, for left and right eyes.

in each eye. Because of the asymmetrical locations of the cataracts within the dilated pupils, the clear regions furthest from the nose (temporal) were wider and larger than those closest to the nose (nasal; Fig. 1a, left).

In adults with normal pupils, receptors are aligned towards the pupil centres, where light is brightest[2,3]. They are aligned there from birth and remain so for life[2]. As part of a wider characterization of his visual system[1], we noted that P.D.'s photoreceptors were aligned with the larger, temporal clear regions in each eye. We made this discovery when P.D. spontaneously reported that point sources of monochromatic red laser light presented in the temporal clear regions appeared distinctly "brighter and whiter". Differences in the brightness and colour of light entering the pupil from different points are termed Stiles–Crawford effects of the first and second kind (SCE I and SCE II), respectively[4,5], and reflect the alignment of cone photoreceptors[2,6]. These effects result from the waveguide properties of photoreceptors, which endow them with directional selectivity for incident light[2].

P.D.'s decision to have his cataracts removed gave us a unique opportunity to test the proposal that cones are actively phototropic, dynamically maintaining alignment with the brightest region of the pupil[7–10]. This was because surgery would shift the brightest regions of his pupils from the temporal margins to the centres (Fig. 1a, middle). The right cataract was removed six weeks after the left one.

We measured SCE I functions across the central horizontal pupil meridians every day after surgery[1]. Figure 1b shows that the peaks of the SCE I functions migrated nasally to the pupil centres over a 10-day period. The left-eye peak moved 1.6 mm, equivalent to 4° of receptor realignment. The right-eye peak moved further (2.6 mm, 6.5°) but did not entirely re-centre, stabilizing instead 0.6 mm to the temporal side. On this evidence, photoreceptors seem to be phototropic (Fig. 1a, right).

P.D. had two separate entry points for light in each eye before surgery — could there have been a concomitant dual photoreceptor alignment, with a minority of receptors aligned with the smaller, nasal clear regions? We failed to find support for this idea, as adapting lights presented to the two clear regions had no differential effect on sensitivity[11], suggesting that the receptors all had a common alignment; moreover, the spread of SCE I function (an index of receptor disarray[6]) was normal and did not decrease after surgery.

The rate of photoreceptor realignment was proportional to the distance remaining to the pupil centres. The dashed curves in Fig. 1b are exponentials that fit best with 5-day time constants for both eyes. Thus, the biophysical processes that underlie phototropism may be under the control of a simple feedback signal. In plants, phototropism is mediated by differential growth[12]. In eyes, it may be that differential longitudinal growth mediated by actin filaments or microtubules makes each photoreceptor phototropic[8,13]. If this is correct, then our analogy with sunflowers is not trivial.

Harvey S. Smallman*†,
Donald I. A. MacLeod*, Peter Doyle‡
**Department of Psychology, University of California at San Diego, La Jolla, California 92093, USA*
†Pacific Science and Engineering Group, San Diego, California 92122, USA
e-mail: smallman@pacific-science.com
‡Department of Mathematics, Dartmouth College, Hanover, New Hampshire 03755, USA

1. Fine, I., Smallman, H. S., Doyle, P. & MacLeod, D. I. A. *Vision Res.* (in the press).
2. Enoch, J. M. & Lakshiminarayanan, V. J. in *Visual Optics and Instrumentation* (ed. Charman, W. N.) 280–309 (CRC, Boca Raton, Florida, 1991).
3. Laties, A. M., Liebman, P. & Campbell, C. *Nature* **218,** 172–173 (1968).
4. Stiles, W. S. & Crawford, B. H. *Proc. R. Soc. Lond. B* **112,** 428–450 (1933).
5. Enoch, J. M. & Stiles, W. S. *Optica Acta* **8,** 329–358 (1961).
6. Applegate, R. A. & Lakshminarayanan, V. *J. Opt. Soc. Am. A* **10,** 1611–1623 (1993).
7. Bonds, A. B. & MacLeod, D. I. A. *Invest. Ophthalmol. Vis. Sci.* **17,** 754–761 (1978).
8. Applegate, R. A. & Bonds, A. B. *Invest. Ophthalmol. Vis. Sci.* **21,** 869–872 (1981).
9. Enoch, J. M. & Birch, D. G. *Phil. Trans. R. Soc. Lond. B* **291,** 323–351 (1981).
10. Kono, M. *et al. Vision Res.* **41,** 103–118 (2001).
11. MacLeod, D. I. A. *Vision Res.* **14,** 369–374 (1974).
12. Dennison, D. S. in *Encyclopedia of Plant Physiology, New Series* (eds Haupt, W. & Feinlib, M. E.) 506–566 (Springer, Berlin, 1979).
13. Laties, A. M. & Burnside, B. in *Motility and Cell Function* (eds Pepe, F., Nachmias, V. & Sanger, J. W.) 285–298 (Academic, New York, 1979).

Palaeoceanography

Antarctic stratification and glacial CO_2

One way of accounting for lowered atmospheric carbon dioxide concentrations during Pleistocene glacial periods is by invoking the Antarctic stratification hypothesis, which links the reduction in CO_2 to greater stratification of ocean surface waters around Antarctica[1,2]. As discussed by Sigman and Boyle[3], this hypothesis assumes that increased stratification in the Antarctic zone (Fig. 1) was associated with reduced upwelling of deep waters around Antarctica, thereby allowing CO_2 outgassing to be suppressed by biological production while also allowing biological production to decline, which is consistent with Antarctic sediment records[4]. We point out here, however, that the response of ocean eddies to increased Antarctic stratification can be expected to increase, rather than reduce, the upwelling rate of deep waters around Antarctica. The stratification hypothesis may have difficulty in accommodating eddy feedbacks on upwelling within the constraints imposed by reconstructions of winds and Antarctic-zone productivity in glacial periods.

To suppress deepwater upwelling around Antarctica, it is necessary either to weaken the westerly wind stress sufficiently in the latitude band of Drake Passage to eliminate the northward flow (Ekman drift) of surface waters, or to counteract this northward drift through southward surface-eddy transport[5]. The first possibility does not seem feasible for glacial periods: the Ekman drift across 55° S is ~25 Sv (1 Sv = 10^6 m^3 s^{-1}; ref. 6) today, and was almost certainly greater during glacial periods because of stronger winds, as expected from the increased Equator-to-Pole temperature gradient and supported by the increased transport of sea salt to the Antarctic continent[7]. This conclusion probably holds even if the latitude of maximum westerly winds shifted slightly towards the Equator, as Sigman and Boyle speculate[3].

The second possibility is also problematic if the glacial Antarctic surface ocean was more stratified than today: eddy transports are thought to scale in proportion to the degree of baroclinicity, which is measured by the slope and spacing of the isopycnal surfaces. High baroclinity favours vigorous eddy transport, whereas low baroclinicity (that is, stratified conditions) suppresses eddy transport[8]. Today, the Antarctic deep upwelling and associated net northward surface flow is estimated to be ~10 Sv, on the basis of geochemical constraints on the partitioning of deep